



# Ocean tides in the Asian semiencllosed seas from TOPEX/POSEIDON

P. Mazzega and M. Bergé

Unité Mixte de Recherche 39 / Groupe de Recherche de Géodésie Spatiale, Toulouse, France

**Abstract.** The eight leading ocean tides (M2, S2, N2, K2, K1, O1, P1, and Q1) have been mapped in Asian semiencllosed seas by inverting combined sets of tide gauge harmonic constants and a reduced set of TOPEX/POSEIDON satellite altimeter data. The tidal maps are given on a  $0.5^\circ \times 0.5^\circ$  grid with their formal error estimates. Numerical experiments conducted in the South China Sea have shown the inverse solutions to be quite insensitive to changes in the parameters of the a priori covariance functions for both the tidal signals and data residual errors. Once the various parameters of the inversion scheme are fixed, the algorithm is applied to the Sea of Okhotsk, the Sea of Japan, the "East China" Sea (including the Bo Hai and Yellow Seas) and the Indonesian Seas. A set of tide gauge constants, not used in our solutions, is then used for comparison. Though these accuracy estimates may be biased because of the uneven stations coverage, we conclude that the inversion of only 21 cycles of TOPEX/POSEIDON data leads to solutions with an accuracy comparable to the Schwiderski (1980b, c) semiempirical model and the Cartwright and Ray (1990) model derived from Geosat altimetry.

## 1. Introduction

Accurate models of the main ocean tidal constituents are ever more required by several observational as well as theoretical developments of geophysics. Since about 10 years it has been recognized that with the aim of reaching the needed accuracy, such models could not rely on the knowledge of the tidal astronomical potential and governing hydrodynamical equations only: direct observations of the tidal fields, up to now mainly in the form of tidal heights data, should be used to constrain the models. The semiempirical model produced by Schwiderski in 1980 [Schwiderski, 1980a] is the best example of a linearized hydrodynamical model with internal parameters adjusted in order to reach a better fit with a large set of coastal tide gauge data [Schwiderski, 1980b, c].

Nowadays, satellite radar altimeters provide a huge amount of measurements of the instantaneous ellipsoidal height of the sea surface, all over the world ocean and during periods of several years. Among other signals and noises, the altimeter datum includes the total tide. As much skill has to be developed for extracting the ocean tides, it was only quite recently that satellite altimetry has achieved results comparable to theoretical modeling. Thus Cartwright and Ray [1990] obtained from the sole analysis of Geosat altimeter data a global model of the diurnal and semidiurnal complex admittances with an accuracy perhaps of the same order of that of the Schwiderski model for the leading waves. During the same decade, assimilation or inverse methods have provided a rigorous theoretical frame to constrain the hydrodynamical models with observations [Bennett and McIntosh, 1982; Zahel, 1991; Jourdin, 1992].

The preliminary sea surface variabilities deduced from the TOPEX/POSEIDON mission unequivocally attest the high quality of the data from the two altimeters, the unprecedented accuracy of the reference radial orbits, and the progresses made in the various geophysical models used for corrections of the raw data. For the purpose of tidal studies, one has to analyze the longest possible time series of measurements so that the results presented in this issue should be considered as preliminary. Nevertheless, the incentives for trying to obtain the tidal heights from TOPEX/POSEIDON are numerous as will appear below.

Before moving to the global inversion of TOPEX/POSEIDON data, we have decided to make numerical experiments at a relatively low computational cost, in domains of limited extensions. The Asian semiencllosed seas are particularly interesting for our purpose. From a dynamical point of view, the tidal patterns are complex with several amphidromic systems and strong gradients of the tidal ranges due to local resonances (see Ye and Robinson [1983] for a discussion of the tidal dynamics in the South China Sea). As a consequence the tidal regime may be predominantly diurnal or even mixed, a peculiarity difficult to grasp with linearized dynamical models, the friction and advection terms being almost equally driven by both semidiurnal and diurnal tidal velocity fields. From a phenomenological point of view, tides in these seas bear strong loading effects, as can be seen, for example, in the numerous gravity loading measurements taken in the vicinity of some of these seas [Endo, 1985; Sun, 1992]. We also dispose of a rather large set of harmonic constants as derived from tide gauge measurements [International Hydrographic Office (IHO), 1979], divided into those to be inverted together with satellite altimetry and those kept independent for models comparisons, as explained in the next section. The third section gives an overview of the inversion scheme. The various numerical tests performed in the South China Sea are presented in section 4, and then final results obtained in all the basins are presented in section 5. The overall performances of our inverse solutions and of the Schwiderski [1980a] and Cartwright and Ray [1990] models

are discussed in section 6. Then options are taken for a prospective global inverse ocean tide model from tide gauge and TOPEX/POSEIDON data.

## 2. Data Preprocessing

### Tide Gauge Harmonic Constants

The tide gauge (hereinafter TG) data used in this study are harmonic constants of the tidal waves as stored in the International Hydrographic Office data bank [IHO, 1979], the phases being referred to Greenwich. In a given area of interest, each station for which the eight leading tides (namely, M2, S2, N2, K2, K1, O1, P1, and Q1) are given is used to prepare the data set to be inverted. The other stations, where some of these constituents are not known, are used to constitute an "external" set for model comparisons and accuracy assessments. The choice of this criterion for separating inverted data from test data allows us to put an homogeneous constraint on all the tidal waves to be recovered though keeping a relatively meaningful data set for comparisons. On the other hand, a possible drawback is to leave large coastal areas sampled by satellite altimetry only (with a relatively slack coverage along the cross-track direction) where the tidal signal may be characterized by short wavelengths.

Some of the TG stations being redundant or just a few kilometers apart, for each tide we average the harmonic constants available in the same  $0.5^\circ \times 0.5^\circ$  predefined mesh (after conversion of the amplitudes and phases into real and imaginary parts). Though a bit wide for coastal areas, this averaging is done in agreement with the grid resolution of the inverse solutions. The averaged constants are assigned to the center of the corresponding mesh. This preliminary processing is done for both the inverted data set and the "external" data set. Only one more constraint was applied to prepare the external set: each station with a distance less than  $0.5^\circ$  from a TG station entering the inverted set has been automatically rejected. This constraint reinforces the independence between the test data set and the inverse solution. Indeed, the mapping of the a posteriori covariance function associated with an inverse solution shows that the model errors are correlated over less than half a degree around the locations of the inverted tide gauge stations [e.g., Jourdin *et al.*, 1991, Figure 5].

The distributions of both TG data sets are plotted with the M2 inverse solution on Figure 1a for the South China Sea. As will be discussed in section 3, this TG distribution can be fruitfully compared with the associated map of the solution formal error map drawn on Figure 2a obtained when inverting TG data only. For the other seas, TG stations are plotted together with the inverse solutions on Figures 3a-3d. The distributions of the inverted TG data are very uneven (see, for example, the Sea of Okhotsk on Figure 3a or the Indonesian Seas on Figure 3c, etc.) or sparse (see, for example, the western coast of the Yellow and East China Seas, Figure 3d). The only exception is the region of the Indonesian Seas where 76 TG stations constitute our external data set. Their distribution is very regular and we have omitted to draw them together with the M2 solution on Figure 3c. Where available, the coastal TG data will bring the stronger local constraints to the inverse solutions. But anywhere else, even in some coastal regions, satellite altimetry only will provide the necessary

information for tidal mapping. The distribution of the external TG data set will be discussed when evaluating the solutions' accuracy.

### TOPEX/POSEIDON Data

Cycles 2 to 22 of TOPEX and POSEIDON altimetry, spanning 210 days of observations, have been extracted over the Asian semiencllosed seas from the CD Rom data bank prepared by the AVISO Group [AVISO, 1992]. The raw data have been reduced for the radial orbit component [Nouel, 1992], the mean sea surface heights [Basic and Rapp, 1992], the wet and dry atmospheric effects, the ionospheric influences with the Bent's model and for the solid tides of an elastic Earth predicted on the basis of the Cartwright and Edden [1973] potential. A constant value of 21 cm was added to the TOPEX altimeter measurements in order to compensate for the relative calibration bias between TOPEX and POSEIDON radar altimeters. No further corrections were investigated for improving the altimeter data set before inversion. Though some of these options may seem quite conservative, they surely fulfil our requirements for this preliminary study.

The distance between the satellite tracks being generally much larger than the along-track data spacing, we keep one datum in 10, following the time ordering of the individual samples. But it should be noted that in several straits (e.g., along the western coast of the Sakhalin Island) and gulfs (e.g., the Bo Hai Sea, the Gulf of Tongking) we have so few and short satellite tracks that the tidal solutions will be estimated from TG data only when available, or even from mere extrapolation from the more open basins.

## 3. Outlines of the Inversion Scheme

As the theoretical background underlying our inverse method of heterogeneous data analysis has already been presented in detail elsewhere [e.g., Mazzega and Jourdin, 1991; Jourdin *et al.*, 1991], we shall here just outline our algorithm based on the generalized least squares criterion [Moritz, 1980; Tarantola, 1987].

The unknowns of the problem are the harmonic constants of the eight leading tidal waves to be mapped on a regular grid. The TG data we use are obviously direct measures of the unknowns at the station locations. A reduced altimeter datum is a linear combination of these unknowns multiplied by time dependent coefficients determined by the respective frequencies and astronomical arguments of the partial tides. When the predicted solid tide is removed from an altimeter datum, the remaining tidal signal is composed of the ocean tide plus a loading vertical displacement. Without resorting to global convolution integrals with the loading Green's function as kernel and the ocean tide itself as input, the loading effect can be approximated with about a 0.5-cm accuracy, by a simple proportionality relation from the local ocean tide. This discrepancy between the proportionality and integral estimates of the loading may reach 3 cm in some coastal regions (see Francis and Mazzega [1990] for a global comparison of the two estimates; see also Wagner [1991]). For saving computational time, we still have kept the proportionality relationship, this contribution being directly included in the observation equation for altimetry.

Smoothing weak constraints are specified on the inverse solutions by introducing a priori covariance functions.

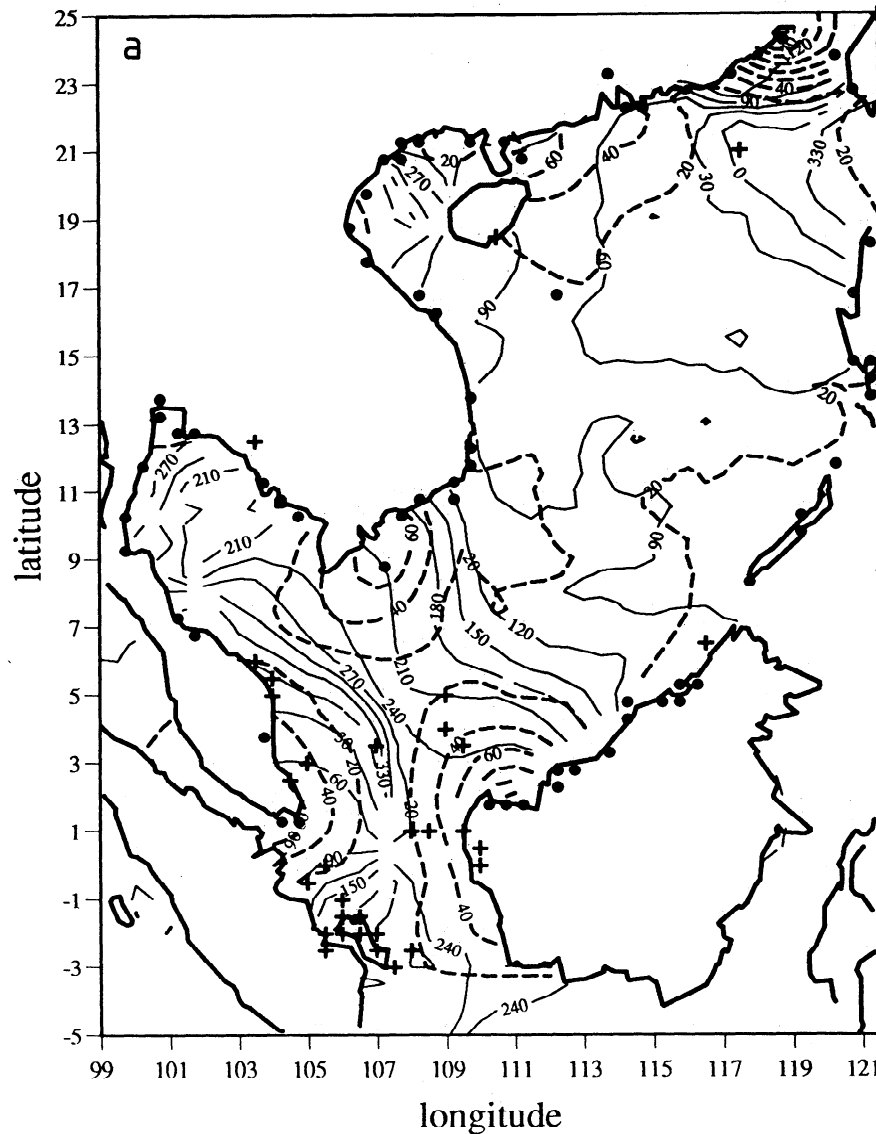


**Figure 1.** (a) M2 inverse solution obtained from tide gauge (TG) and TOPEX/POSEIDON data in the South China Sea (isoamplitudes: 20 cm; isophases: 30°). Dots indicate the locations of the reinterpolated TG stations used in the inversion; pluses those of the TG used for model comparisons. (b) K1 inverse solution (isolines: 10 cm; 30°).

Differing from a mere assimilation scheme where the smoothing constraints are enforced by the equations of tidal dynamics (and their adjoint [see *Bennett, 1992*]), we rely on parameterized stationary covariances deduced from the globally averaged power spectrum of a preliminary tidal solution (here the Schwiderski model; see *Mazzega and Jourdin [1991]* for details). It should be kept in mind first that an infinite set of cotidal maps may fit the same power spectrum (or equivalently covariance function) and second that this a priori information is a weak constraint: the inversion of a large and accurate enough data set would lead to a solution completely independent from the choice of the a priori constraints.

The complete a priori information on the tidal signal spans a covariance tensor where the cross covariances between waves of different species or between the real and imaginary parts of any tide are set to zero. Damped cosine functions are

fitted to the remaining tidal covariances obtained from the Schwiderski model. In the numerical tests to be described below, we keep as variable parameters of the analytical covariance functions, the tidal variances, the distances for which the functions reach their first zero ("zero-crossing" parameters) and the characteristic distances for exponential damping ("e-folding" parameters).

The space-time characteristics of the noises or correction residual errors of the TG and altimeter data are also specified a priori by parameterized covariance functions. Table 1 gives an overview of the functional dependences and parameters of the covariances used in our inversion scheme.

The inverse tidal maps are built up as linear combinations of the data. Using the least squares criterion [e.g., *Tarantola 1987*], the optimal data coefficients are obtained from the various covariances and inverse of the matrix of weighted normal equations (see *Mazzega and Jourdin [1991]* for details).

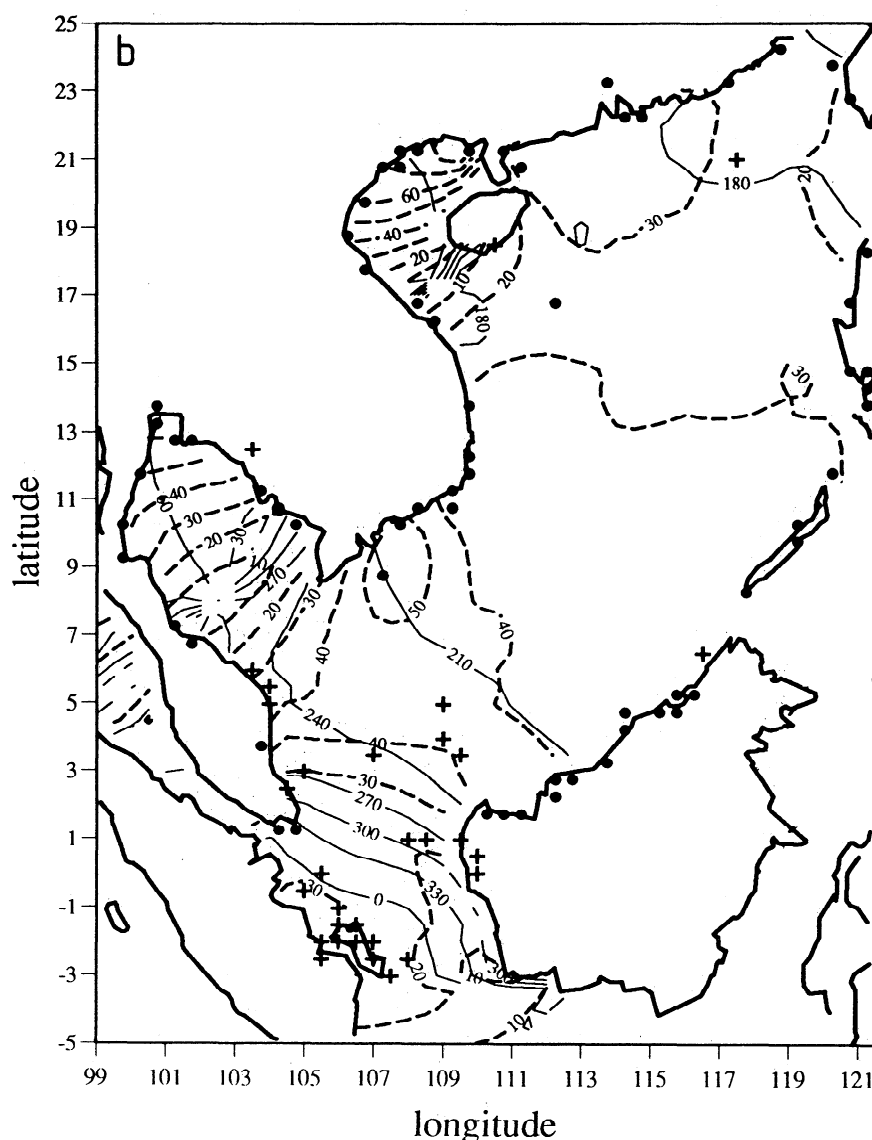


Figure 1. (continued)

In this algorithm, each datum virtually contributes to each unknown, whatever may be their relative distance so that we have to proceed to the numerical resolution of very large symmetric nonnegative definite full systems. The main incentive for such an approach was to try to separate on a global scale the quite large radial orbit error (with typical wavelengths of 20, 000 km) from the more regional oceanographic signals. With the available computational resources, we must reduce the data set before handling such problems. An alternative consists in solving a suboptimal problem where only the nearest data from the (running) solution location are inverted. With the high-accuracy reference orbits now available for TOPEX/POSEIDON, we here decide to adopt this strategy in which a set of linear equations has to be solved for each node of the solution grid. All the data in a radius of about 2 spherical degrees around the considered node are inverted (with typically 1500 to 2000 altimeter and TG data). Among all the TG stations available in a given spherical cap, only the 10 nearest ones are retained for a point inversion, mainly in order to reduce the averaging process near the coasts.

The reference solutions are mapped with their formal standard deviations on a  $0.5^\circ \times 0.5^\circ$  grid. The various tests presented in the next section are performed with a degraded resolution of only  $1^\circ \times 1^\circ$ . Though the tidal covariance tensor also accounts for the waves Mf, Mm and Ssa (these constituents are also in the total tide observed by altimeters), we here only map semidiurnal and diurnal constituents.

#### 4. Inversion Tests in the South China Sea

The tides of the South China Sea present interesting features, with semidiurnal waves propagating southward from the Luzon Strait (opened on the Pacific) down to the Gulf of Thailand through amphidromic systems, and strong amplifications of the diurnal waves in the Gulf of Tongking and Gulf of Thailand. We also have a quite homogeneous distribution of the TG data available for inversion as can be seen on Figure 1a. Moreover, the relatively limited extension of the basin allows for intensive explorations of the capabilities of the inversion algorithm itself through in turn perturbations of the analysis internal parameters as explained below.

**Table 1.** Summary of the Functional Dependences and Parameters of the Various Covariances Entering the Inversion Algorithm (Based on the generalized least squares Criterion)

	Analytical Covariance Function	Standard Deviation, cm	Correlation Length $l$ Zero-Crossing $z$ Correlation Time $t$
Semi diurnal tides	damped cosine	26	$l=13^\circ$
Diurnal tides	---	11	$l=17^\circ$
Long-period tides	---	3	$l=25^\circ$
Altimeter noise	Dirac delta	3	
Radial orbit error	damped cosine	20	1 cycle/day $t = 2$ days
Residual MSS	damped cosine	7	$l = 2^\circ$ $z = 1^\circ$
Mesoscale variability	damped cosine	10	$z = 1^\circ$ $t = 25$ days
Residual geophysical correction	damped cosine	30	$l = 15$ $z = 7^\circ$ $t = 5$ days

#### Tests Relative to the a Priori Information

For a given choice of the set of covariance functions we compute the inverse tidal solutions on a  $1^\circ \times 1^\circ$  grid. It first appears that too high a priori variances of the residual mean sea surface (MSS) or residual geophysical correction can lead to quasi-singular least squares matrices. In the case of the MSS, two altimeter measurements nearly colocalized and taken a long time period apart will induce a high value of their MSS covariance "far" from the diagonal of the least squares matrix.

Similar situations are generated when considering the covariance of the geophysical residual correction for pairs of distant altimeter measurements (the space and time correlation lengths being fixed to about 5-7 degrees and 5 days, respectively; see *Benveniste* [1989] for the rationale of this choice). For some threshold of the signal (i.e., tides) to noise (i.e., nontidal components of altimeter data) ratio, this kind of matrix being only slightly diagonal dominant will have a very bad conditioning. Except for these extreme situations, we have run the algorithm with 11 different sets of covariance parameters, changing only one of them in turn. A summary of the parameters controlling these tests is given in Table 2.

In the first three numerical experiments we have multiplied the typical distances of the  $e$ -folding and zero-crossing of the full tidal covariance tensor by factors 1, 1/2 and 1/3 (to simplify, we just give an overall "correlation length" for tides in Tables 1 and 2). The first case corresponds to the globally averaged tidal correlation lengths as deduced from the Schwiderski model (together with our stationarity and isotropy assumption): these correlation lengths are typically 13 degrees and 17 degrees for the semidiurnal and diurnal waves, respectively. Though one should not interpret these correlation lengths as characteristic wavelengths of the dynamic tides, we still expect the tidal heights to be correlated over much shorter distances in the often very shallow semiencllosed seas (much power being transmitted from the long wavelengths to shorter ones). The conclusion drawn from these tests is that the inverse solutions of all the tidal constituents are only marginally sensitive to the choice of the a priori tidal covariance lengths. The discrepancies between the different inverse solutions always remain lower than the a posteriori formal errors. In the same way the solutions are not significantly changed when increasing the a priori tidal variances by a factor of 2 (test 4 of Table 2), or when further setting to zero the cross covariances between tides of the same species (test 5). This last test shows that the inverted data set brings enough observational information to discriminate between the different tidal constituents.

**Table 2.** Numerical Values of the Parameters Perturbed in Turn in the Inversion Tests Performed in the South China Sea

Test	Tidal Covariances	Orbit Error Variance	Residual MSS Variance	Ocean Variability Variance	Residual Correction Variance	Altimeter Noise Variance
1	Sf= 1/1	400	49	100	900	9
2	Sf= 1/2	400	49	100	900	9
3	Sf= 1/3	400	49	100	900	9
4	Vf= 2	400	49	100	900	9
5	Vf= 2 cross= 0	400	49	100	900	9
6	Sf= 1/2	400	16	16	900	9
7	Sf= 1/2	16	49	100	900	9
8	Sf= 1/2	400	16	100	900	9
9	Sf= 1/2	400	49	16	900	9
10	Sf= 1/2	400	49	100	16	9
11	Sf= 1/2	400	49	100	400	16

Our reference inverse solutions are computed on the basis of the parameters given as test 11. All variances are given in  $\text{cm}^2$ . The tidal covariances are modified by the following factors: Sf is a scale factor applied to the correlation lengths given in Table 1; Vf is a factor applied to the variances; cross=0 indicates that all the cross correlations are set to zero.

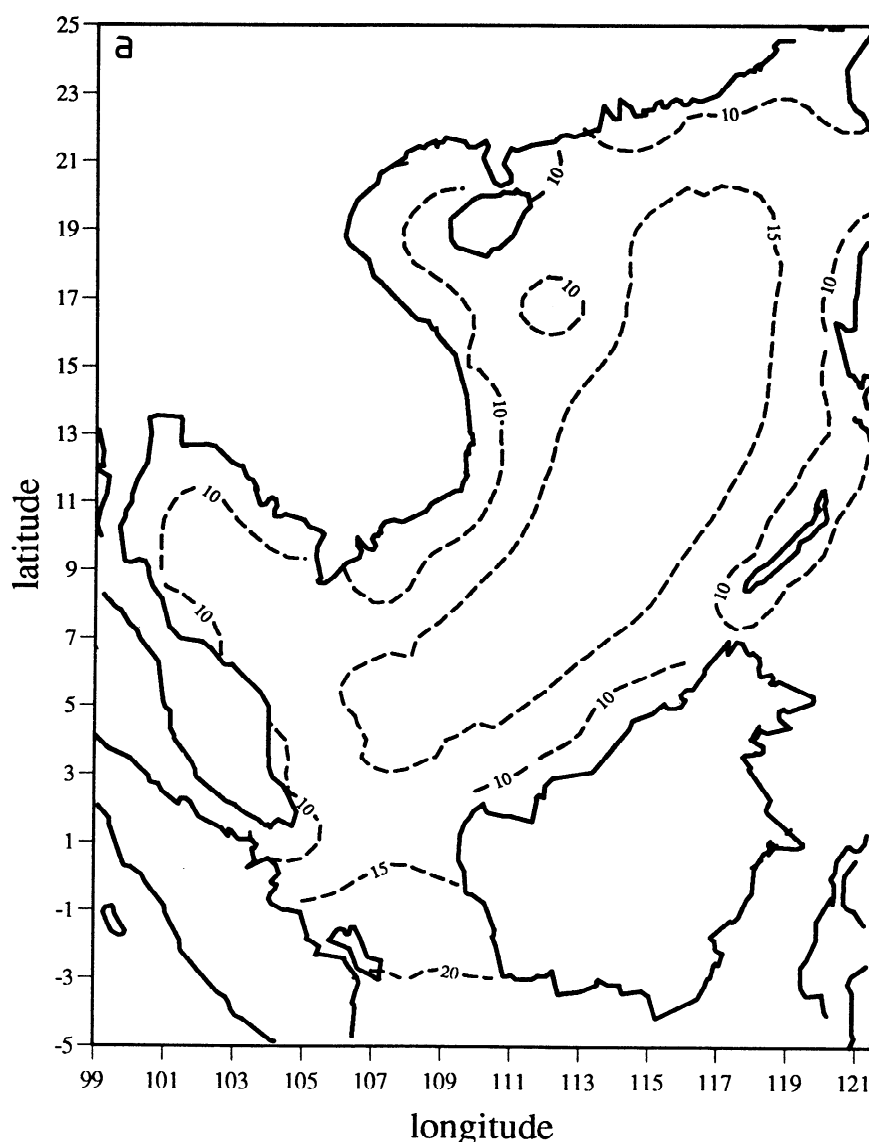


**Figure 2.** (a) Map of the formal error estimates (isolines: 5 cm) associated with the M2 solution (real part) obtained by the inversion of tide gauge data in the South China Sea (see Figure 2a for their distribution). The error is about 5 cm near the coasts. (b) Same as Figure 1a but when inverting a combined set of tide gauge data and 210 days of TOPEX/POSEIDON altimetry (isolines: 2 cm).

We then in turn perturb the a priori variances of the radial orbit error, MSS residuals, ocean mesoscale variability, geophysical correction residuals, and altimeters noise (tests 7 to 11 in Table 2). Some simultaneous perturbations have also been tried (see tests 6 and 11 of Table 2). The conclusions are the same as previously quoted: the induced solutions perturbations are only marginally significant with regard to the formal error estimates.

In order to locate these areas of maximum sensitivity of the solutions, we have computed a map of the RMS of the departures between the solutions corresponding to tests 1 to 10 relative to the solution of test 11 (that will constitute our reference algorithm configuration in the tidal mapping; see below). As may be expected, the main solution changes (of about a few centimeters for M2 or K1) take place: (1) where we have almost no data or only very short altimetric tracks (as, for example, between Singapore, Sumatra and Borneo where no TG data are inverted); (2) where the wave dynamics are

noticeably complex, as, for example, south of the peninsula of Vietnam for M2 (with a very local maximum of 9 cm RMS) or west of the Hainan Dao island, in the Gulf of Tongking for K1 (up to 4 cm RMS).

#### Tests Relative to the Data Contents

Tidal solutions and formal error estimates have been also computed by inverting TG data only, TOPEX/POSEIDON altimetry only, and then the combined data set. Figures 1a and 1b depict the inverse solutions for M2 and K1, respectively, obtained with the combined data set.

The maps derived from the TG data alone present amplitudes too high by 2 or 3 dm in the middle of the basin. In fact, the tidal correlation lengths are large enough to allow for a direct interpolation of the harmonic constants, for example, between the coasts of Vietnam and Sarawak. At the same places the formal error maps give maximum values of up to 20

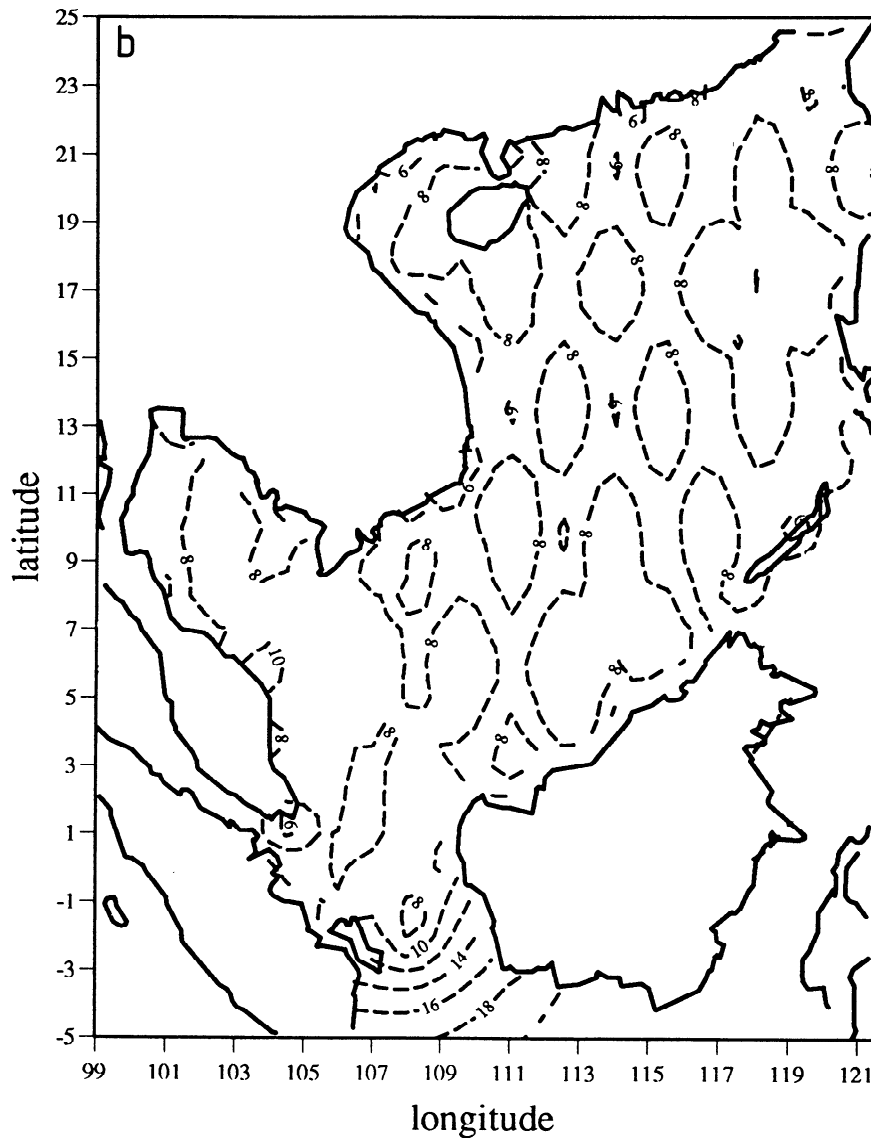


Figure 2. (continued)

cm for M2 ( 1 standard deviation; see Figure 2a) and 7 cm for K1. At the TG station locations, the formal error reaches the 2-cm level attributed as the a priori data standard deviation for a single tidal wave.

The representativeness of some TG data used in these inversions may be questionable. Several stations are located in harbors or even up rivers (note that the dots in Figure 1a indicate the station positions after relocation by our averaging process as explained above, and not those of the original coastal sites). A prior estimate of the representativeness of a given TG datum would necessarily rely on an a priori tidal model [Kagan and Kivman, 1994]. Assuming our prior knowledge on tides being the null state (except for the tidal covariances), we choose here to invert all the available data without discrimination. The possible influence of a nonrepresentative data on the basin-wide solutions should be mostly tempered by nearby TG data or altimetric data.

When inverting altimetry alone, our algorithm tends to oversmooth the strong tidal gradients near the coasts or in the gulfs. In the middle of the basins the amplitudes and phases are

well restored. The formal error maps show diamond-shaped patterns, with, for M2, 7-cm minima at the crossover points, and 10-cm maxima between tracks. These errors rapidly increase when moving away from the well-sampled regions (say, south of the equator). It may also reach up to 15 - 20 cm at the coastline.

The inversion of the combined set gives solutions with the right amplitudes and phases in midbasin and also includes the gradients in the gulfs and narrow seas (see Figures 1a and 1b). Indeed, both type of data bring complementary information necessary to map the complex tidal patterns. The error maps are a mixture of the diamond-shaped iso-contours in the "open" sea and error decreases near the coasts where TG data are available (see Figure 2b for M2). All these comments extend to the eight tidal constituents without change (except of course for the values of the formal errors, these being smaller for less energetic waves).

All these tests clearly show that the combined set of satellite altimetry and TG data are accurate and dense enough to determine the solutions well in most parts of the South China Sea so that the choice of the covariances parameters have a



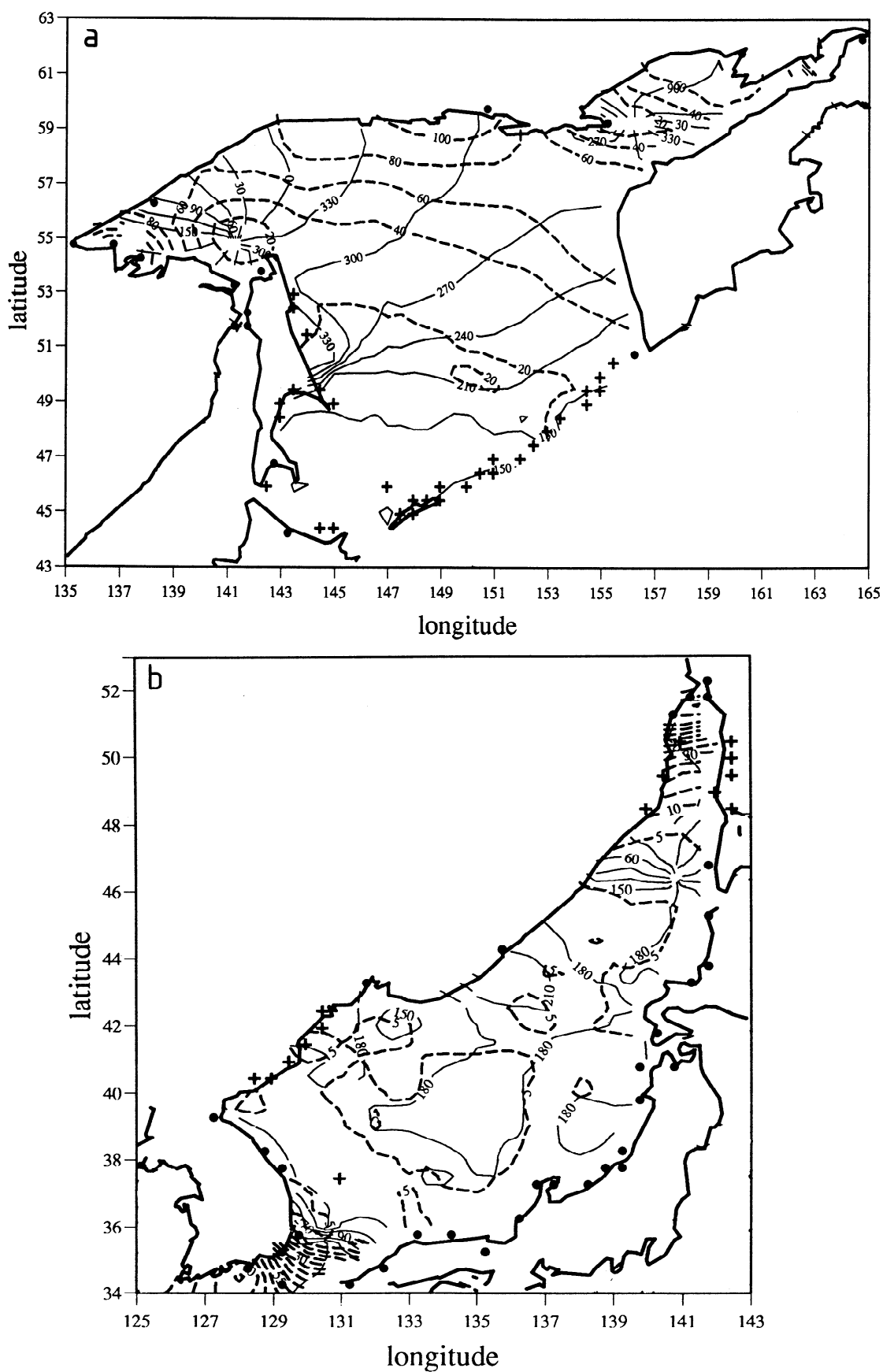


**Figure 3.** M2 inverse solutions for the Sea of Okhotsk (Figure 3a; isolines: 20 cm, 30°), Sea of Japan (Figure 3b; 5cm, 30°), Indonesian Seas (Figure 3c; 20 cm, 60°), East China Sea (Figure 3d; 20 cm, 30°). Reinterpolated TG locations are indicated by dots when inverted, by pluses when used for model comparisons.

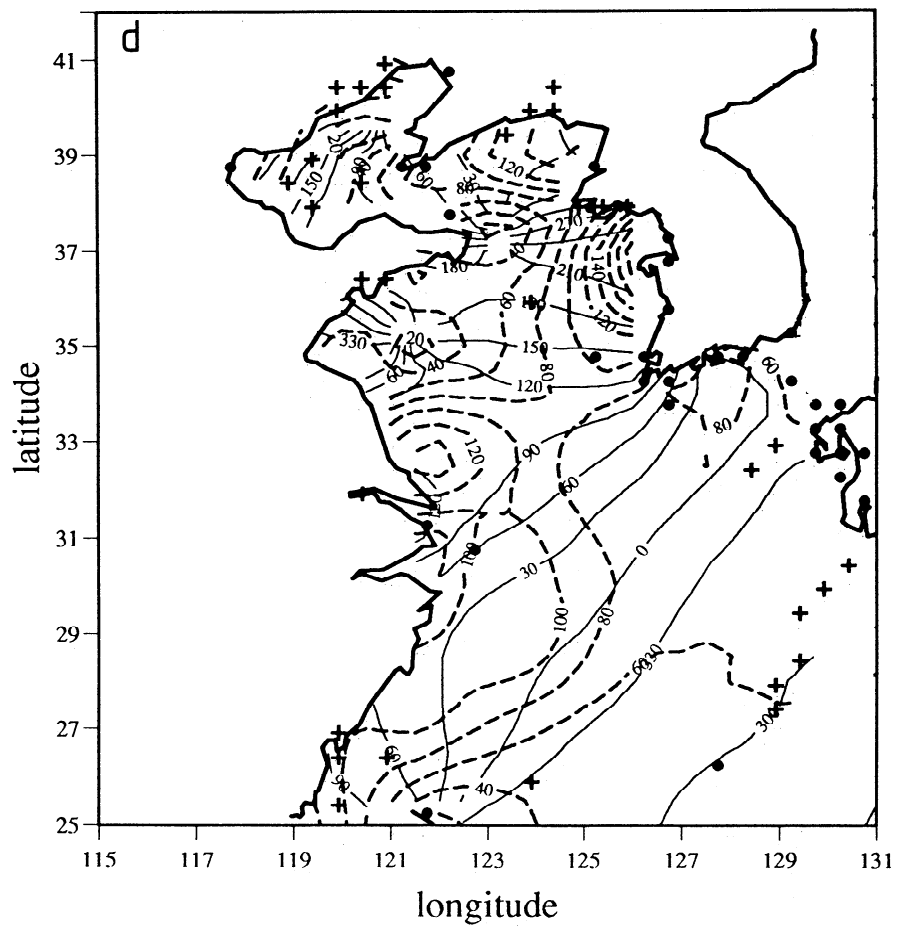
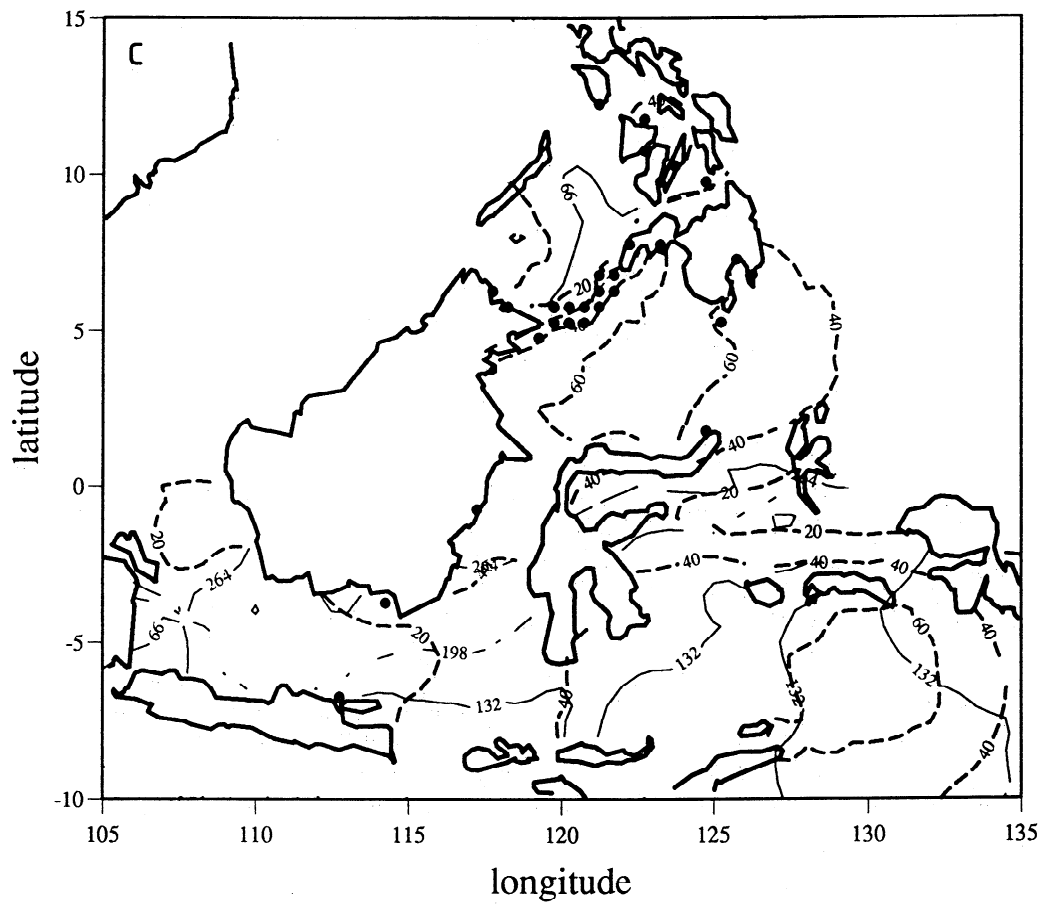
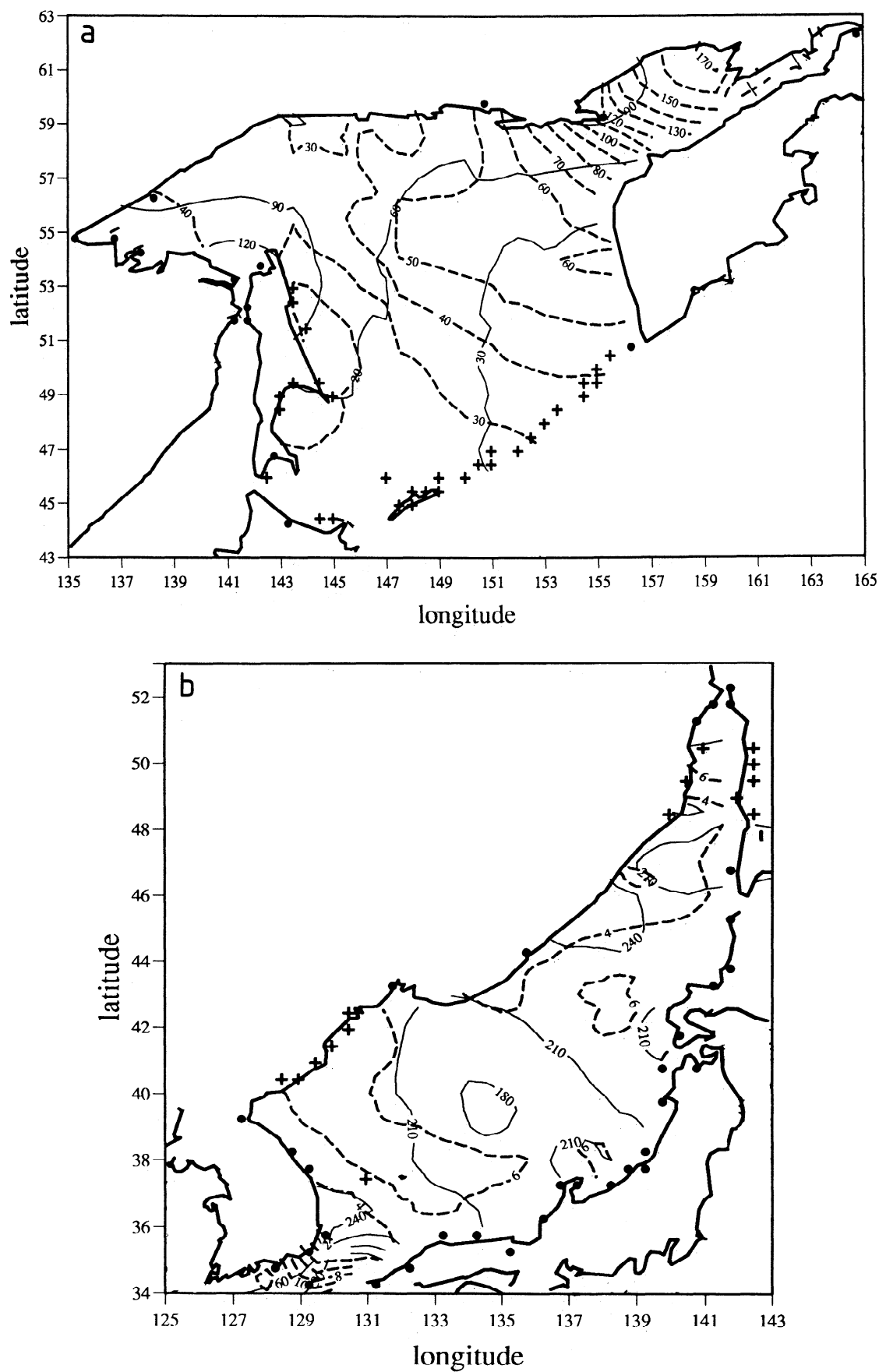
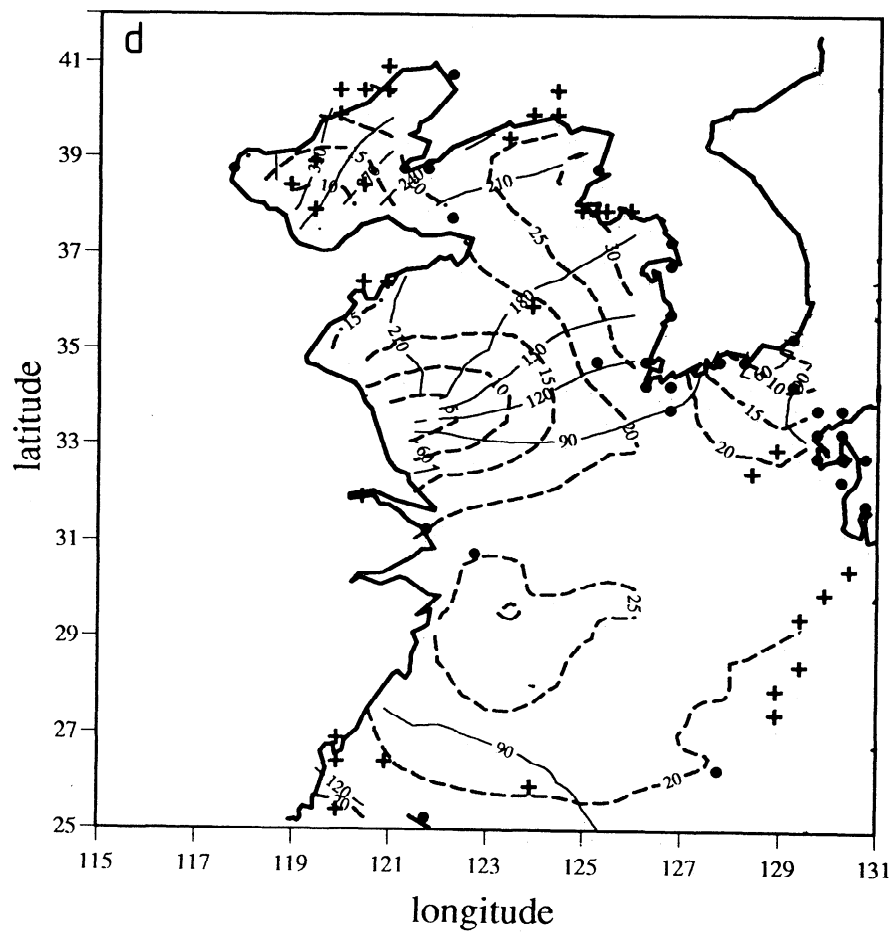
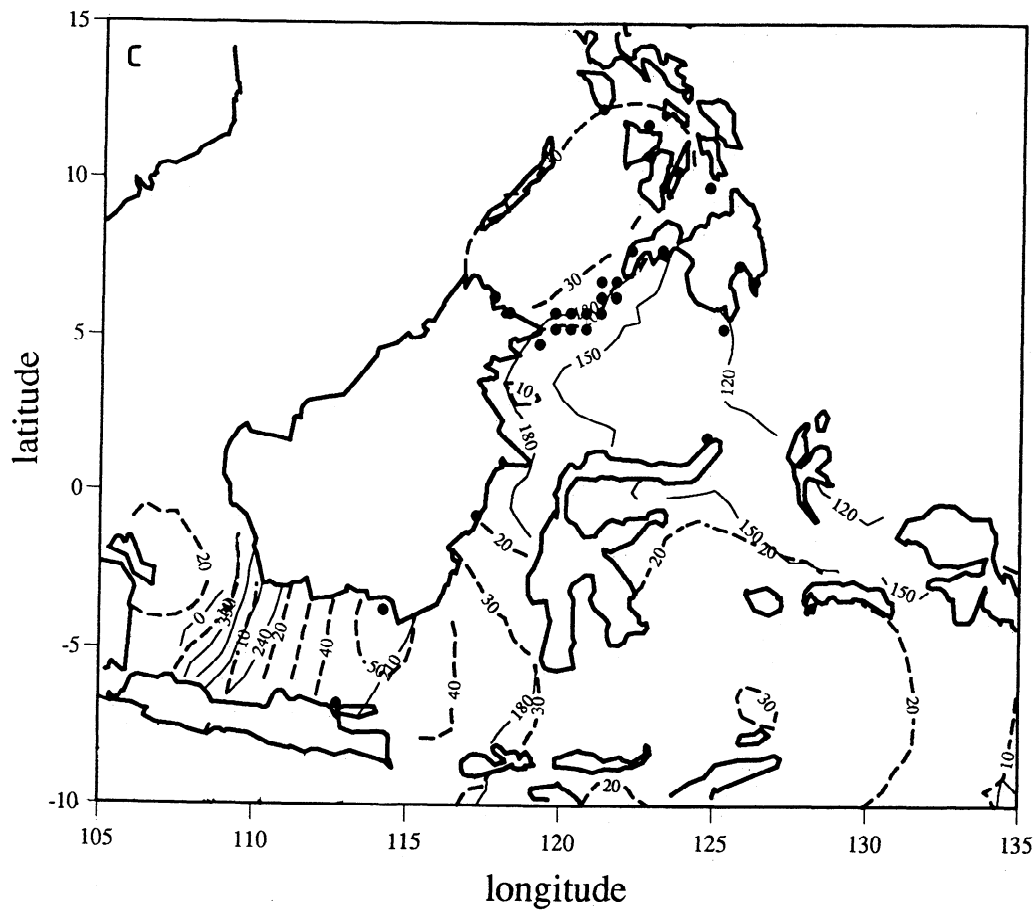
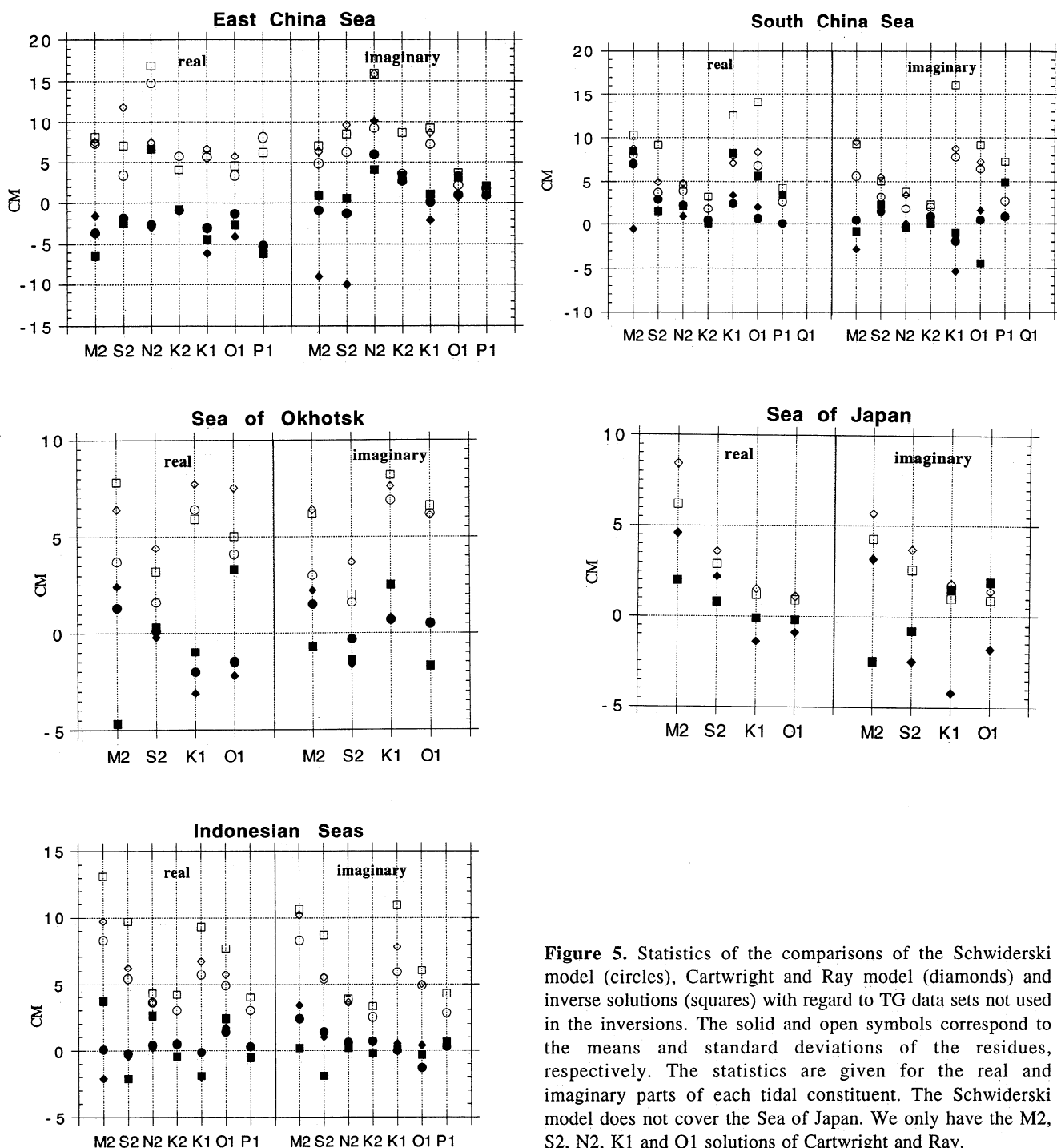


Figure 3. (continued)



**Figure 4.** Same as Figures 3a-3d but for the K1 tide (isolines are (a) 10 cm, 30°, (b) 2 cm, 30°, (c) 10 cm, 30°, (d) 5 cm 30°). Reinterpolated TG locations are indicated by dots when inverted, by pluses when used for model comparisons.





**Figure 5.** Statistics of the comparisons of the Schwiderski model (circles), Cartwright and Ray model (diamonds) and inverse solutions (squares) with regard to TG data sets not used in the inversions. The solid and open symbols correspond to the means and standard deviations of the residues, respectively. The statistics are given for the real and imaginary parts of each tidal constituent. The Schwiderski model does not cover the Sea of Japan. We only have the M2, S2, N2, K1 and O1 solutions of Cartwright and Ray.

weak influence on the tidal maps. Moreover, the information brought on ocean tides by TG stations and satellite altimetry is complementary when tidal dynamics is very complex as in these shallow seas.

## 5. Tidal Solutions and Model Comparisons in the Asian Seas

The various parameters of the set of signal and errors covariance functions are now fixed to the values headed as test 11 in Table 2. Just for control, the TG and TOPEX/POSEIDON data sets are first inverted separately. The same

complementarity of the two data sets is observed in each basin (note that due to the sparseness of TG data, the solution mainly relies on satellite altimetry in the Sea of Okhotsk). Then we proceed to the computation of our so-called "reference" solutions on the basis of the combined data set. The tidal solutions for the eight leading constituents are computed for each semiclosed sea independently, on a  $0.5^\circ \times 0.5^\circ$  grid, together with their formal error estimates (in real and imaginary parts).

We here only present the cotidal maps for the M2 (Figures 3a-3d) and K1 (Figures 4a- 4d) waves. The order of magnitude

**Table 3.** Statistics of the Residues Obtained When Comparing the Schwiderski Model, the Cartwright and Ray Model and the Inverse Solutions With the Tide Gauge Data Used in Our Inverse Solutions

South China Sea		Schwiderski		Cartwright & Ray		Inverse Solution	
		Mean	RMS	Mean	RMS	Mean	RMS
M2	real	2.3	7.7	-0.9	8.8	1.7	3.4
	imaginary	-1.3	7.9	-0.1	11.2	-0.1	4.5
S2	real	-1.3	6.3	-0.5	7.1	0.0	2.8
	imaginary	-1.9	8.7	-1.1	7.8	0.3	3.6
N2	real	-2.0	4.4	-1.7	3.5	0.1	2.3
	imaginary	0.3	6.8	0.4	6.4	0.0	1.6
K2	real	-0.1	3.5			0.0	1.2
	imaginary	-0.7	2.9			-0.1	1.5
K1	real	-0.6	6.8	-0.7	7.8	-0.3	3.7
	imaginary	-0.4	8.4	-2.5	10.7	-0.5	4.5
O1	real	2.9	9.2	0.1	8.2	-0.5	4.5
	imaginary	-0.2	6.4	-0.6	5.8	0.9	5.3
P1	real	-0.2	2.7			0.1	2.2
	imaginary	-0.1	3.5			-0.3	1.9
Q1	real	-0.6	2.7			0.0	1.5
	imaginary	0.3	2.7			0.3	1.5

This comparison should not be used for model qualification purpose (see text).

of the formal errors associated with these maps is the same as observed in the test basin (see Figures 2a-2b), the shape of the isocontour patterns reflecting the heterogeneous data coverage in each sea. The tidal dynamics and energy budget being mainly controlled by the velocity fields (that we cannot estimate without resorting to hydrodynamics), we shall not try to comment on these purely empirical solutions obtained from height measurements.

The Schwiderski [1980b, c] model and the Cartwright and Ray [1990] and inverse solutions exhibit similar tidal patterns in the various basins. Beyond this qualitative agreement, these models may present considerable localized discrepancies. For example, in the South China Sea, considering any pair of models, the amplitude of the (complex) discrepancies is about 5-10 cm in the northern basin but reaches 10-20 cm south of 10° N and in the Gulf of Thailand. With about 1 m departures between each other, the three models are even completely conflicting in the narrow strait between Taiwan and China. Our inverse solution is surely wrong between Sumatra and Borneo as can be checked by comparison with the external TG data set (this deficiency is accounted for in the statistics given below). Indeed, owing to the specified a priori covariances of the altimeter nontidal components ("noises"), the satellite profiles are too short to allow for a proper decorrelation of the tides, and we do not retain TG data on the southern coasts of Borneo (Figure 1a) where the tidal gradients are strong. The three models also disagree by 25-45 cm in a narrow zone centered on 8°N, 107°E which corresponds to the location of an inverted pelagic datum. We presently have no criterion to decide between this

datum being spurious, or the Schwiderski and Cartwright and Ray solutions being locally too smooth (these two models still presenting up to 25 cm departures in this region). On the whole, our inverse solutions better agree with the Schwiderski model in the different basins, probably because of the common use of numerous TG data.

We then proceed the comparison of all these solutions with the "external" TG data sets. As explained previously, these data are not used in our inverse solutions nor in the Cartwright and Ray [1990] solutions. However the bulk of them has been hydrodynamically interpolated in the Schwiderski [1980c] model via the algorithm described in his paper. So the accuracy estimates (for Schwiderski) obtained from these comparisons may be strongly biased.

Considering only the M2 tide, the numbers of available TG stations for comparison are 26 in the South China Sea, 10 in the East China Sea, 28 in the Sea of Okhotsk, 14 in the Sea of Japan and 76 in the Indonesian Seas. All the constituents are not given at these stations so the statistics are sometimes evaluated on even more reduced data sets. This situation may lead in particular to abnormally high values of the mean of the residues. Another problem comes from the very uneven geographical distribution of these TG data, as can be seen by a quick inspection of the maps given in Figures 1a and 3a, 3b and 3d. In the Sea of Okhotsk, for example, the test TG data set only covers the eastern coast of the Sakhalin Island and the Kouriles Island arc. Almost no data at all are available far from the coasts.

So our statistics probably do not reflect the overall accuracy of the different models. Nevertheless, we do not have other

independent in situ observations to go further in these comparisons. Only the gravity loading measurements could be used for this purpose (with specific difficulties and trends) but the computations of the gravity loading effects for each model would be required, a task we have not undertaken in this study.

For each TG station and each constituent, we have linearly interpolated over four surrounding points the amplitudes and phases given by each model. The residues with regard to the in situ data are computed on the real and imaginary parts. We then compute for each basin the mean and standard deviation of the residues. Note that Schwiderski's model does not cover the Sea of Japan. Moreover, we presently only have at our disposal the M2, S2, N2, K1, and O1 maps of the *Cartwright and Ray* [1990] model.

The means and standard deviations so obtained are sketched in Figure 5. We first observe that each model may present relatively high mean departures with regard to the comparison data sets. As long as these abnormal values involve just one tidal model over three, we interpret them as a failure of the corresponding model rather than being an artifact of our biased estimate. The overall performance of Schwiderski model is quite satisfactory. This good agreement probably results from the hydrodynamical interpolation (and smoothing) of most of these data in his solution. Comparing the altimeter derived solutions, we see that the *Cartwright and Ray* model achieves better performance in the South China Sea and Indonesian Seas, while the inverse solutions derived from TOPEX/POSEIDON seem to be slightly better in the Sea of Japan. The TG data we invert in the Indonesian Seas are gathered in the north of the Celebes Sea. No data are available in the southern basins for tempering the far extrapolation of these data. So we believe this extremely unbalanced distribution to be responsible for the relatively unsatisfactory results obtained with our algorithm in this region. We have found no explanation for the high standard deviations of our K1 solutions in the Indonesian Seas and South China Sea. The performances of the altimeter-derived models are very comparable in the Sea of Okhotsk and East China Sea.

In summary, for these Asian seas, the three models seem to be of equivalent accuracies, with slight preferences to be given to one of them when considering a specific basin. This statement should still be considered with care, the test data sets presenting very uneven geographical coverages of the various basins. It has been shown in particular that quite large regional or local discrepancies between these models can remain unsampled and smoothed out from the residues statistics when performing comparisons with in situ data.

## 6. Discussion and Conclusion

The previous discussion about these preliminary results provides important constraints for refining our data preprocessing and inversion algorithm. Much longer TOPEX/POSEIDON altimeter time series are now available. So we shall perform global inversions following these guidelines.

Comparing in the world ocean the *Schwiderski* [1980b, c] model and the *Cartwright and Ray* [1990] model with the pelagic tidal constants recently compiled by *Smithson* [1992], we have verified these two solutions to be of almost the same accuracy (at least for the five leading waves) as we

also observe here in the Asian semiencllosed seas [see *Wagner*, 1991; *Mazzega et al.*, 1993]. This test may still be slightly vitiated as Schwiderski used some of the near-shore deep sea measurements in his hydrodynamical interpolation (these stations were quoted in the preliminary reports distributed with the model tapes). Though their solution noticeably lacks smoothness in dynamically active regions of the ocean, the results obtained by *Cartwright and Ray* are encouraging when considering that these authors were able to recover the tidal signal from a set of Geosat data, with a relatively high level of the radial orbit error (based on the GEM T2 Earth's gravity field model). The exploiting of their method of data analysis on a long enough time series of TOPEX/POSEIDON altimetry is very promising.

The global solutions we have obtained on the same Geosat data set (though we kept as reference the even less accurate GEM T1 radial orbit) is, on the contrary, too smooth over the continental shelves and seas of limited extension [*Mazzega et al.*, 1993]. We have shown this (partial) failure of our previous inverse modeling to result from both the heavy error budget of the Geosat data and the strongly reduced data sets used for each individual solution (at that time we were performing only global matrix inversions built on about 6000 altimetric data each). These two basic limitations of our previous inversion strategy resulted in too strong a priori constraints relative to the data content.

The preliminary results obtained in this paper from the data inversions have an accuracy comparable to that of the two other models used for comparison. The choice to invert numerous regional data sets rather than once for all very large systems is obviously a better strategy, in particular when the radial orbit error is below the level of the tidal signal. In fact, a much larger data set can be analyzed in this way. But the key point is that we should get even better results when inverting longer time series of TOPEX/POSEIDON altimetry. During the 210 days of observations analyzed here the M2 tide has only three apparent oscillations and other waves are hardly distinguished from each other. The present success of our inversions mainly relies on the overall accuracy of the TOPEX/POSEIDON data and surely not on the ease of separating the different lines of the tidal spectrum. This last improvement will come with longer altimetric time series.

More care will also be taken when correcting the raw altimetric data. The corrections applied here are based on very conservative assumptions. Using better correction models will leave much smaller residuals characterized by lower variances and correlation scales. This situation will ease the tidal signal recovery, even along relatively short altimetric tracks in semiencllosed or shallow water seas.

We also have to reconsider the availability of coastal TG data. We first notice that the accuracy achieved by the Schwiderski models is largely due to the huge "assimilation" of an extended set of such data. Second, it appears that in numerous extended coastal regions (see, for example, the Sea of Okhotsk and the eastern coast of the East China Sea in Figures 3a and 3d; the same kind of situation occurs, for example, on the coast of the Patagonian shelf), only short TG recordings have been performed from which only four to six waves were determined. All the TG sets used here for comparison were in this category.

Going along this line, we have compared the three tidal models with the TG data used in our inversion and then estimated the associated statistics, exactly as was performed in

the previous section. The results, summarized in Table 3, should clearly not be retained as a qualification of our inverse solutions. Indeed, we can virtually get any desired degree of agreement between an inverse solution and its data set just by a proper reduction of the associated data error variance. Looking at the inverse solutions, we see that the mean departures are extremely low. The a posteriori standard deviations are larger than the error associated a priori to the input TG data (2 cm RMS), showing that the inversion is a smoothing filter. The standard deviations of both other models relative to the data are about twice as large as those obtained with the inversion. These trends are systematically observed in each basin. This result clearly shows that a given degree of accuracy (typically a few centimeters) can only be achieved by using tide gauge data where the tidal dynamics is complex.

For all these reasons we have decided to further include in the global inversion to be performed the TG stations with a limited number of waves. The pelagic tidal constants and the tidal gravity loading constants will be kept independent for model comparisons.

If the TOPEX/POSEIDON could be followed on by similar satellite altimeter missions over one or two decades, the absolute accuracy of the global tide models may be improved over the centimeter level and tens of other tidal constituents with typical amplitudes of a few centimeters may also be accurately mapped and made available for other research fields in oceanography and geophysics.

**Acknowledgments.** These computations have been performed partly on the CRAY 2 of the Météorologie Nationale (MN Toulouse) and partly on the CRAY YMP now available at the Centre National d'Etudes Spatiales (CNES Toulouse). We are particularly indebted to CNES for without its constant support, since several years, these studies could not be achieved. We are grateful to Pierre Féménias and Eric Jeansou (both working under temporary contract at GRGS) for their spontaneous help in extracting TOPEX/POSEIDON data from CD-Roms. P.M. would like to thank Laetitia Pineda for her kind help in the (otherwise tedious) tabulation of some results presented here. The comments given by two anonymous reviewers have been helpful in preparing the final version of this paper.

## References

AVISO, AVISO User Handbook: Merged TOPEX/POSEIDON products, *Rep. AVI-NT-02-101-CN*, 2nd ed., Centre National d'Etudes Spatiales, Toulouse, France, 1992.

Basic, T., and R.H. Rapp, Ocean wide prediction of gravity anomalies and sea surface heights using GEOS 3, Seasat and Geosat altimeter data, and ETOPO5U bathymetric data, *Rep. 416*, Dep. Geod. Sci. and Surv., Ohio State Univ., Columbus, 1992.

Bennett, A.F., *Inverse Methods in Physical Oceanography, Monographs on Mechanics and Applied Mathematics*, Cambridge University Press, Cambridge, 346 pp., 1992.

Bennett, A.F., and P.C. McIntosh, Open ocean modeling as an inverse problem: Tidal theory, *J. Phys. Oceanogr.*, **12**, 1004-1018, 1982.

Benveniste, J., Observer la circulation des océans à grande échelle par

altimétrie satellitaire, thèse Univ. Sci. Toulouse, 198 pp., Toulouse, France, 1989.

Cartwright, D.E., and A.C. Edden, Corrected tables of tidal harmonics, *Geophys. J. R. Astron. Soc.*, **33**, 253-264, 1973.

Cartwright, D.E., and R.D. Ray, Oceanic tides from Geosat altimetry, *J. Geophys. Res.*, **95**, 3069-3090, 1990.

Endo, T., An experimental study of regional heterogeneities of gravity tides in central Japan, *Bull. Earthquake Res. Inst. Univ. Tokyo*, **60**, 39-86, 1985.

Francis, O., and P. Mazzega, Global charts of ocean tides loading effects, *J. Geophys. Res.*, **95**, 11411-11424, 1990.

International Hydrographic Office (IHO), Tidal constituents bank; station catalog, Rep. of the Ocean and Aquat. Sci., Dep. Fish. and Oceans, Ottawa, Ont., 1979.

Jourdin, F., Assimilation de mesures marégraphiques et altimétriques dans un modèle hydrodynamique de marées océaniques, thèse Univ. Sci. Toulouse, 241 pp., Toulouse, France, 1992.

Jourdin, F., O. Francis, P. Vincent, and P. Mazzega, Some results of heterogeneous data inversions for oceanic tides, *J. Geophys. Res.*, **96**, 20267-20288, 1991.

Kagan, B.A., and G.A. Kivman, A necessary condition for the representativeness of island tidal measurements, *J. Geophys. Res.*, in press, 1994.

Mazzega, P., and F. Jourdin, Inverting Seasat altimetry for tides in the NE Atlantic: Preliminary results, in *Tidal Hydrodynamics*, edited by B. Parker, pp. 569-592, John Wiley, New York, 1991.

Mazzega, P., O. Francis, and M. Bergé, OMP1: An inverse model of the global ocean tides, *Proc. 12th Intern. Symp. on Earth Tides*, 4-7 Aug. 1993, Beijing, China, in press.

Moritz, H., *Advanced Physical Geodesy*, 500 pp, H. Wichmann Verlag, Karlsruhe, Germany, 1980.

Nouel, F. (Ed.), Validation des éphémérides précises TOPEX/POSEIDON, *Note Tech. Int. CNES, TP-RP-41, 7072 CN*, Centre National d'Etudes Spatiales, Toulouse, France, 1992.

Schwiderski, E.W., On charting global ocean tides, *Rev. Geophys.*, **18**(1), 243-268, 1980a;

Schwiderski, E.W., Ocean tides, I, Global ocean tidal equations, *Mar. Geod.*, **3**, 161-217, 1980b.

Schwiderski, E.W., Ocean tides, II, A hydrodynamical interpolation model, *Mar. Geod.*, **3**, 219-255, 1980b.

Smithson, M.J., Pelagic Tidal Constants, *IAPSO Publ. Sci.* **35**, 191 pp., Bidston, England, 1992.

Sun, H.P., Comprehensive researches for the effect of the ocean loading on gravity observations in the western Pacific area, *Bull. Inf. Marées Terr.*, **113**, 8271-8292, 1992.

Tarantola, A., *Inverse Problem Theory. Methods for Data Fitting and Model Parameter Estimation*, 613 pp., Elsevier, Amsterdam, 1987.

Wagner, C.A., How well do we know the deep ocean tides ? An intercomparison of altimetric, hydrodynamic and gage data, *Manuscr. Geod.*, **16**, 118-140, 1991.

Ye, A.L., and I.S. Robinson, Tidal dynamics in the South China Sea, *Geophys. J. R. Astron. Soc.*, **72**, 691-707, 1983.

Zahel, W., Modeling ocean tides with and without assimilating data, *J. Geophys. Res.*, **96**, 20379 - 20391, 1991.

M. Bergé and P. Mazzega, UMR39/GRGS/CNES, 18 Avenue Edouard Belin, 31055 Toulouse Cedex, France. (e-mail: ciamp@mfn.cnes.fr)

(Received November 12, 1993; revised June 30, 1994; accepted June 30, 1994.)